Journal of Photochemistry and Photobiology A: Chemistry 279 (2014) 1–7

Contents lists available at ScienceDirect

Journal of Photochemistry and Photobiology A: Chemistry

journal homepage: www.elsevier.com/locate/jphotochem

Uniform TiO_2/In_2O_3 surface films effective in bacterial inactivation under visible light

Francesca Petronella[a,b], Sami Rtimi[a,*], Roberto Comparelli[b], Rosendo Sanjines[c], Cesar Pulgarin[a,*], M. Lucia Curri[b], John Kiwi[d]

[a] Ecole Polytechnique Fédérale de Lausanne, EPFL-SB-ISIC-GPAO, Station 6, CH-1015 Lausanne, Switzerland
[b] CNR-IPCF, Istituto per i Processi Chimico Fisici, U.O.S. Bari, c/o Dip. Chimica, Via Orabona 4, 70126 Bari, Italy
[c] Ecole Polytechnique Fédérale de Lausanne, EPFL-SB-IPMC-LNNME, Bat PH, Station 3, CH-1015 Lausanne, Switzerland
[d] Ecole Polytechnique Fédérale de Lausanne, EPFL-SB-ISIC-LPI, Bat Chimie, Station 6, CH-1015 Lausanne, Switzerland

ARTICLE INFO

Article history:
Received 2 September 2013
Received in revised form 6 January 2014
Accepted 13 January 2014
Available online 23 January 2014

Keywords:
TiO_2/In_2O_3
Magnetron sputtering
Bacterial inactivation
IFCT mechanism

ABSTRACT

This study shows that the surface modification of TiO_2 is an effective route to increase the TiO_2 absorption in the visible region up to ~600 nm for photocatalytic applications. The In_2O_3 decorated TiO_2 films on polyester obtained by reactive sputtering were shown to accelerate the *Escherichia coli* inactivation under actinic and simulated solar light. TiO_2 sputtered films for 10 min inactivated bacteria within 300 min under actinic light. The inactivation time was reduced when using a TiO_2 10 min–In_2O_3 10 s sample to 150 min when using actinic light and 90 min by simulated sunlight with 50 mW/cm^2 (one half of AM1). Thinner TiO_2–In_2O_3 coatings led to faster bacterial inactivation compared to thicker TiO_2–In_2O_3 layers due to the reverse diffusion of the generated charges. The increase in the optical absorption of the green coloured TiO_2–In_2O_3 film was a function of the In_2O_3 loading as detected by diffuse reflectance spectroscopy (DRS). Evidence of the lack of TiO_2 lattice doping by the sputtered In_2O_3 was found by X-ray diffraction spectroscopy (XRD). The deconvolution of TiO_2 bands detected by X-ray photoelectron spectroscopy (XPS) revealed the existence of Ti^{4+}/Ti^{3+} signals suggesting redox catalysis at the surface of the TiO_2–In_2O_3. The photo-induced interfacial charge transfer (IFCT) between TiO_2 and In_2O_3 can be accounted for by the band position potentials of both semiconductors. The faster kinetics of TiO_2–In_2O_3 inducing *E. coli* inactivation with a higher quantum efficiency compared to TiO_2 takes place in spite of the low intensity of the IFCT optical absorption bands >400 nm.

1. Introduction

Chemical modification of surfaces, focused on inhibiting or reducing the ability for a microorganism to grow, is an area of topical research interest to reduce microbial contamination responsible of hospital-acquired infections (HAI) [1–8]. The microbes causing HAI have two main properties: most of them are toxic and resistant to antibiotics and they survive for long times on surfaces present in hospital environment [9–14]. The level of contamination of public hospitals in the UK and Switzerland has been found to be higher than the allowed level set for hospital rooms. For example, the contamination of 10^5 CFU/cm^2 was observed in a diabetic wound dressing. Disinfecting surfaces were applied and the microbial density reduced, since bacterial concentration was not high and re-growth of bacteria was not observed [4]. Such observations warrant the investigation of antibacterial surfaces as addressed in the present study. Increasing public concerns drives the research to perform modification of the textiles with nanoparticles at relatively low temperatures in order to achieve materials presenting fast bacterial inactivation kinetics, acceptable adhesion, long-term stability and cost effective. In addition the increasing bacterial resistance to antibiotics in the last decade and the widespread biofilm formation by toxic pathogens spreading bacteria in schools, hospitals and public places motivates the present work on surfaces with antibacterial nanoparticles at relatively low temperatures. The purpose is to prepare disinfecting surfaces with fast bacterial inactivation kinetics, acceptable adhesion and long-term stability.

Indeed, the present study focuses on the preparation, bacterial inactivation kinetics and characterization of TiO_2–In_2O_3 films on polyester fabrics.

Colloidal deposition of nanoparticle semiconductors/metals/oxides on textiles led to mechanically unstable and not reproducible films, presenting low uniformity and poor adhesion, since

* Corresponding authors.
E-mail addresses: sami.rtimi@epfl.ch (S. Rtimi), cesar.pulgarin@epfl.ch (C. Pulgarin).

1010-6030/$ – see front matter © 2014 Elsevier B.V. All rights reserved.
http://dx.doi.org/10.1016/j.jphotochem.2014.01.005

they can be wiped off by a cloth or thumb [15]. Sputtering of semiconductor or metal nanoparticle films is able to load textile and other surfaces and, at the same time, to overcome the shortcomings of colloidal films. Sputtering semiconductors/metals/oxides on non-heat resistant substrates, such as polymer thin film textiles, is performed at temperatures up to 150 °C, which is the temperature limit of most of such substrates.

TiO_2 has been used in bactericide surfaces for the last 30 years and some reviews have detailed the efficiency and mechanism of the charges in this semiconductor leading to bacterial inactivation [16–18]. To extend the optical spectrum of TiO_2 into visible Ag has been used on TiO_2 films [19,20]. Cu also been used in conjunction with TiO_2 for the purpose of accelerating bacterial inactivation under simulated solar radiation as reported in some recent studies [21–23].

The addition of In_2O_3 would also prevent recombination of the e^-/h^+ generated upon irradiation of TiO_2 particles, thus enhancing the formation of highly oxidative radicals on the TiO_2 surface. Such an effect, along with the extension of the In_2O_3 visible absorption up to 600 nm, accelerates the bacterial reaction kinetics [24]. TiO_2–In_2O_3 has been reported as a catalyst for isopropanol decomposition under solar simulated radiation [25,26] and TiO_2–In_2O_3 has been shown effective in the photo-activated degradation of phthalate [27]. Photo-electrochemical measurements have yielded an indirect band-gap for In_2O_3 with values between 2.3 and 3.0 depending on the size and physical state of In_2O_3 [28–29].

The present study addresses the sputtering, bacterial inactivation kinetics and characterization of the nanocomposite TiO_2–In_2O_3 films on polyester fabrics. The In_2O_3 absorption in the visible up to 600 nm is able to shift the activity of TiO_2 to the visible region of the solar spectrum for the prepared samples.

2. Experimental

2.1. Reactive sputtering of films and determination of the coating thickness

The TiO_2 and TiO_2–In_2O_3 thin films were deposited onto polyester in the magnetron chamber by first sputtering Ti and subsequently In from their respective targets in the presence of mixture of Ar and O_2 gases. Before the deposition the residual pressure in the magnetron chamber was $\leq 10^{-4}$ Pa. The distance between substrates, polyester samples of 2 cm × 2 cm, and the targets was kept fixed at 10 cm. The TiO_2 thin films were sputtered by direct magnetron sputtering (DC) using a 5 cm diameter Ti target 99.99 atomic % (KurtJ, Lesker, East Sussex, UK) in an Ar and O_2 atmosphere. The total working pressure $P = (P_{Ar} + P_{O_2})$ was fixed at 0.5 Pa and the ratio $P_{O_2}/P = 4.5\%$. The sputtering current on the Ti target was 280 mA providing a power of 120 W ($U = -450$ V) and a current density of 12.7 mA/cm^2. Pulsed direct magnetron sputtering (DCP) was used to sputter the In_2O_3 and was operated at 50 kHz with 15% reversed voltage. The sputtering power was fixed at 50 W providing a negative voltage of −500 V, and a power of 140 W.

The selected polyester substrates corresponds to the EMPA (Eidgenössische Materialprüfungs und Forschungsanstalt) test cloth sample no. 407, namely a polyester Dacron polyethylene terephthalate type 54 spun, plain weave ISO 105-F04 used for colour fastness determinations. The thermal stability of Dacron polyethylene terephthalate is 115 °C for long-range operation and 140 °C for times ≤1 min. The thickness of the polyester is of 130 nm ± 10%.

2.2. Evaluation of the bacterial inactivation of E. coli and irradiation source

The samples of *Escherichia coli* (*E. coli* K12) was obtained from the Deutsche Sammlung von Mikroorganismen und Zellkulturen GmbH (DSMZ) ATCC23716, Braunschweig, Germany, and were used to test the antibacterial activity of the TiO_2–polyester and TiO_2–In_2O_3 sputtered fabrics. The polyester fabrics, both bare and sputtered ones, were sterilized by autoclaving at 121 °C for 2 h. 20 μL *E. coli* K12 culture aliquots, with an initial concentration of 10^6 to 10^7 CFU mL^{-1} in NaCl/KCl (pH 7) were placed on TiO_2 and TiO_2–In_2O_3 coated as well as on bare (control) polyester fabric. The polyester is a micro-porous substrate and distributes the inoculum evenly on the TiO_2 or TiO_2–In_2O_3 films without needing an adsorption stage. A uniform and non-heterogeneous contact was established between the sample and the well dispersed bacterial solution for all the investigated samples. The exposition of the fabrics to light was carried out at 25–28 °C. The samples were then placed on Petri dishes covered with a lid to prevent evaporation. Afterwards, at scheduled time, each fabric sample was transferred into a sterile 2 mL Eppendorf tube containing 1 mL autoclaved NaCl/KCl saline solution. This solution was subsequently mixed thoroughly using a Vortex for 3 min. Serial dilutions were made with NaCl/KCl solution. An aliquot of 100 μL was pipetted onto a nutrient agar plate and then spread over the surface of the plate using standard plate method. Agar plates were incubated lid down, at 37 °C for 24 h before colonies were counted. Three independent assays were performed for each sputtered textile sample. The actinic irradiation lamp used shown in Fig. 1 as a source of white light is shown in Fig. 1 and was an Osram Lumilux T8-L18W (4.2 mW/cm^2) as is used widely used as indoor source of light in health facilities. The solar simulated light source was a solar simulator (Heraeus, Hannau, Germany) with a light emission between 200 and 800 nm provided for a 100 W Xe-light resembling the solar spectrum with a light intensity of 50 mW/cm^2. This is equivalent to the average solar light dose reaching European countries.

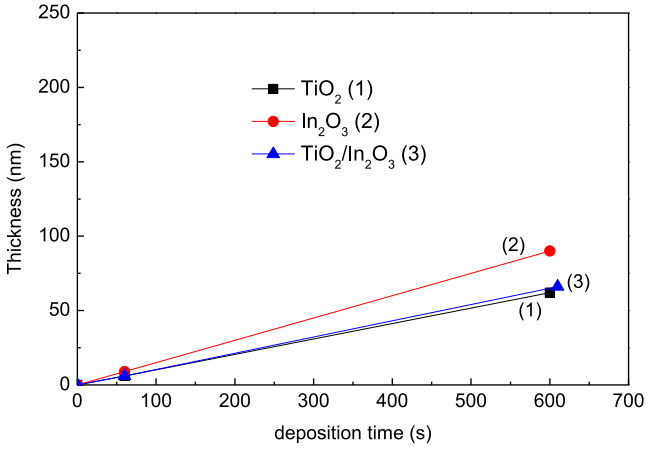

Fig. 1. Thickness calibration for direct current magnetron sputtering (DC) of TiO_2 and pulsed direct current magnetron sputtering (DCP) of In_2O_3 in reactive atmosphere.

2.3. X-Ray fluorescence analysis of samples (XRF)

The TiO_2 and In_2O_3-content on the polyester was evaluated by X-ray fluorescence, by using an RFX, PANalytical PW2400 spectrometer. The results are shown in Table 1.

2.4. Diffuse reflectance spectroscopy (DRS)

Diffuse reflectance spectroscopy on polyester samples was carried out using a Perkin Elmer Lambda 900 UV–vis NIR-spectrometer provided for with a PELA-1000 accessory within the wavelength range of 200–800 nm and a resolution of one nm. The absorption of

Table 1
In_2O_3 and TiO_2 contents as a function of sputtering times determined by X-ray fluorescence (XRF).

Sample	Deposition time	% In_2O_3 wt/wt polyester	% TiO_2 wt/wt polyester
In_2O_3	5 s	0.05	–
	10 s	0.12	–
TiO_2	1 min	–	0.01
	5 min	–	0.04
	10 min	–	0.12
TiO_2/In_2O_3	10 min/5 s	0.06	0.10
	10 min/10 s	0.09	0.09
	10 min/20 s	0.15	0.10
	10 min/40 s	0.18	0.10

the samples was plotted in Kubelka–Munk (KM) arbitrary units vs wavelength.

2.5. X-ray diffraction of TiO_2 and TiO_2–In_2O_3 samples (XRD)

Crystal structures were characterized by X-ray diffraction (XRD) and recorded by means of an X'Pert MPD PRO from PANalytical equipped with a secondary graphite (002) monochromator and an X'Celerator detector operated in Bragg–Brentano geometry. A step size of 0.0081 and an acquisition time of 2 min per degree were selected.

2.6. X-ray photoelectron spectroscopy (XPS)

An AXIS NOVA photoelectron spectrometer (Kratos Analytical, Manchester, UK) equipped with monochromatic Al $K\alpha$ ($h\nu$ = 1486.6 eV) anode was used. The electrostatic charge effects on the samples were compensated by means of the low-energy electron source working in combination with a magnetic immersion lens. The carbon C1s line with position at 284.6 eV was used as a reference to correct the charging effect. The quantitative surface atomic concentration of some elements was determined from peak areas using sensitivity factors [30]. Spectrum background was subtracted according to Shirley [31]. The XPS spectra were analyzed and deconvoluted using CasaXPS-Vision 2 software, Kratos Analytical UK.

3. Results and discussion

3.1. Profilometry

The thickness of the sputtered layers was determined by means of a profilometer (Alphastep500, Tencor) for TiO_2, In_2O_3 and TiO_2–In_2O_3 sputtered films onto silica wafers in the magnetron chamber reactive atmosphere. A 10 min TiO_2 sputtering led to a thickness of 60 nm. Since the average atomic distance between metal particles is ~0.3 nm, each 0.2 nm thick atomic layer about contains 10^{15} atoms/cm^2 [25]. A 50 nm thickness is equivalent to 300 layers and the Ti is being deposited at a rate of 0.5×10^{15} atoms/cm^2 s. Fig. 1 trace 3 shows that the thickness of the TiO_2–In_2O_3 layers after 10 min and 10 s sputtering, is of 55–60 nm, thus suggesting the formation of a TiO_2–In_2O_3 composite. Indeed, the thickness was found lower than the 120 nm expected from the sum of the individual contributions of TiO_2 and In_2O_3 layers. The sample found to lead to the fastest bacterial inactivation TiO_2 10 min–In_2O_3 10 s consisted of 250 layers of TiO_2 and in the surface periphery 3–5 layers In_2O_3.

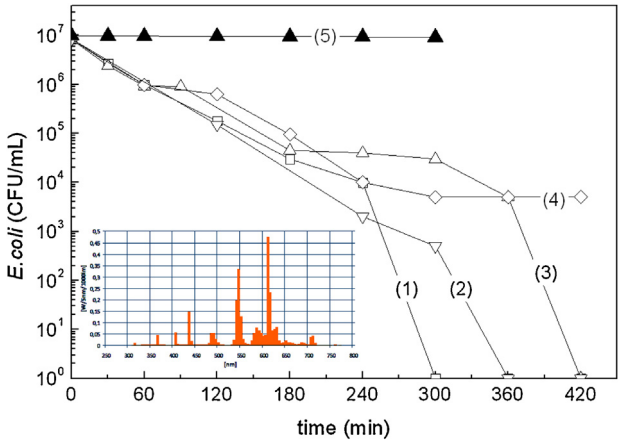

Fig. 2. *E. coli* inactivation kinetics under light irradiation by TiO_2 polyester samples sputtered for: (1) TiO_2 10 min, (2) TiO_2 5 min, (3) TiO_2 1 min, (4) polyester and (5) TiO_2 10 min in the dark. The insert shows the Osram Lumilux T8-L18W (4.0 mW/cm^2) emission spectrum used to photo-activate the samples.

3.2. Bacterial inactivation investigation

Fig. 2 reports the results for the *E. coli* inactivation of TiO_2 polyester samples exposed to an actinic Lumilux T8-L18W light source. The sample sputtered by DC for 10 min (trace 1) led to bacterial inactivation within 300 min. Samples sputtered for 5 min and 1 min did not induce bacterial inactivation in short times, since they did not contain enough TiO_2 and thus needed longer (6 and 7 h for the 5 and 1 min sputtered sample, respectively) inactivation times. Table 1 shows the loading of TiO_2 and TiO_2–In_2O_3 in polyester as determined by X-ray fluorescence. Bare polyester under light irradiation led, to some extent, to bacterial inactivation as shown in Fig. 2, trace 4. Such an effect can be ascribed to the presence of bleaching agents, insecticides and pesticides derived from the polyester manufacturing process. Fig. 2, trace 5 shows a control experiment performed keeping in the dark the 10 min TiO_2 sputtered sample, and resulted in no bacterial inactivation.

A bacterial inactivation time of 2 h for TiO_2 sputtered on cotton for 10 min has been previously reported [22]. However, the experiment was performed with an initial concentration of 10^6 CFU/ml, lower than the 10^7 CFU/ml used in the set of experiments presented in Figs. 2 and 3.

Fig. 3a shows the bacterial inactivation experiments carried out on TiO_2–In_2O_3, TiO_2 and In_2O_3 samples. Fig. 3a, trace 1 shows the inactivation of *E. coli* by a 10 min sputtered sample as a control experiment for the inactivation kinetics of TiO_2–In_2O_3, In_2O_3 samples shown in traces 2–7. The fastest bacterial inactivation was obtained for the TiO_2 10 min–In_2O_3 10 s sputtered sample (Fig. 3a, trace 3). When In_2O_3 was sputtered for longer times (Fig. 3a, traces 4 and 5) the inactivation time became longer. In_2O_3 sputtered on the TiO_2 layer for 20 s and 40 s increased the In_2O_3 thickness leading to a bulk inward diffusion of the e^-–h^+ charge carriers generated in the In_2O_3 [6,19,22]. Trace 6 shows the small bacterial inactivation of In_2O_3 by itself under light suggesting that a synergic interaction with TiO_2 is required to lead to fast bacterial inactivation as shown in Fig. 3a, trace 1. Finally the TiO_2–In_2O_3 semiconductor properties leading to bacterial inactivation are confirmed by the results shown in Fig. 3a, trace 7 since only a low bacterial inactivation was observed in the absence of light irradiation.

The results presented in Fig. 3a, traces 3–5, suggest that longer sputtering times led to samples with larger In_2O_3 particle, thus decreasing the available contact surface with bacteria [23]. In_2O_3 sputtering for 10 s may results in optimal In_2O_3 cluster size, with

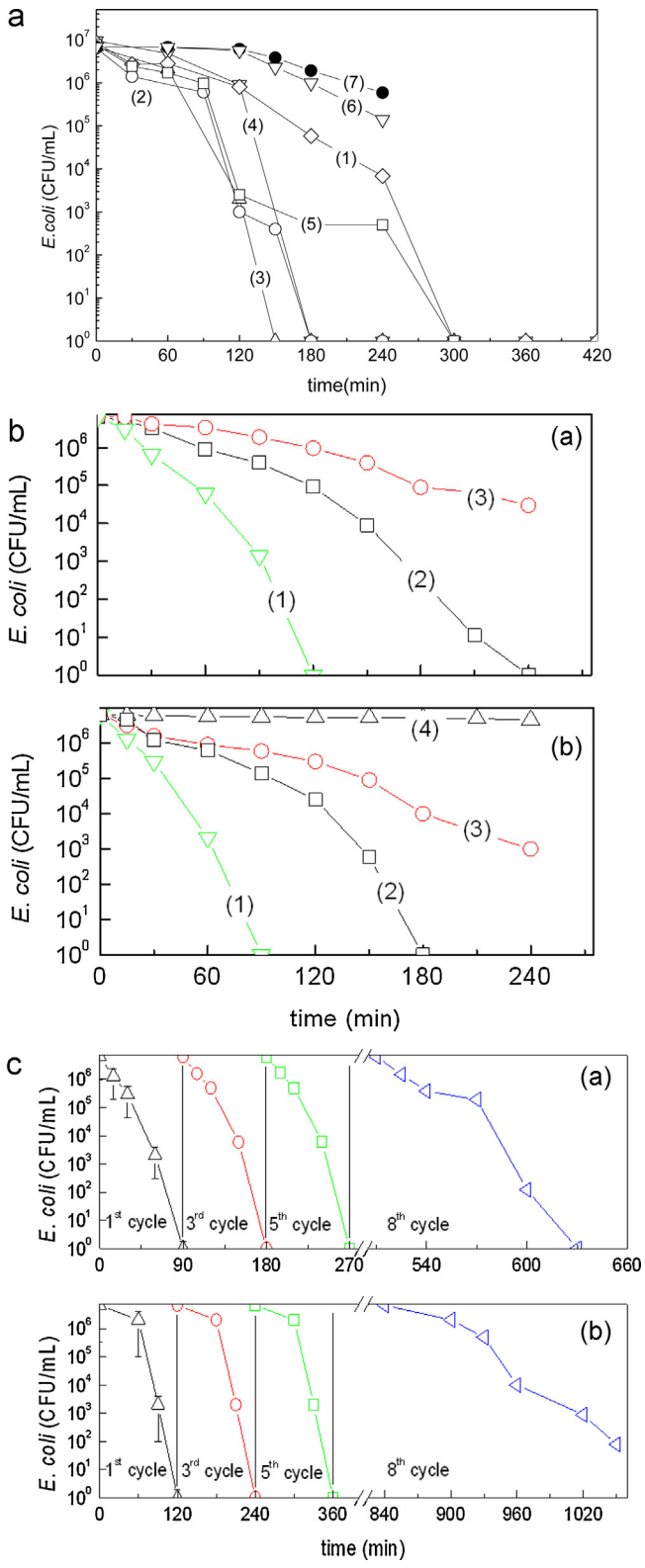

Fig. 3. (a) *E. coli* inactivation on samples under Osram Lumilux T8-L18W lamp (4.0 mW/cm^2) as noted in traces (1)–(6): (1) TiO_2 10 min, (2) TiO_2 10 min/In_2O_3 5 s, (3) TiO_2 10 min/In_2O_3 10 s, (4) TiO_2 10 min/In_2O_3 20 s, (5) TiO_2 10 min/In_2O_3 40 s, (6) In_2O_3 alone and (7) sample TiO_2 10 min/In_2O_3 10 s in the dark. (b) *E. coli* inactivation under solar simulated light for (1) TiO_2/In_2O_3 (sputtered for 10 min/10 s), (2) TiO_2 (sputtered for 10 min), (3) In_2O_3 (sputtered for 10 s) samples, respectively and for (4) a bare polyester sample, at light intensities: a – 30 mW/cm^2 and b – 50 mW/cm^2. (c) *E. coli* inactivation recycling experiments on TiO_2/In_2O_3 sputtered for 10 min/10 s on polyester under irradiation by: a – Suntest solar simulator CPS 50 mW/cm^2 (360–800 nm) and b – Osram Lumilux T8-L18W (4.0 mW/cm^2).

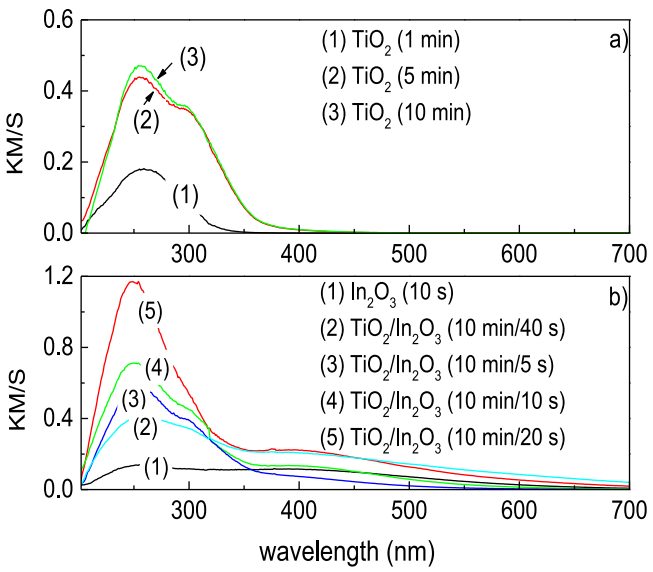

Fig. 4. Diffuse reflectance spectra (DRS) of TiO_2 and TiO_2/In_2O_3 samples in Kubelka–Munk units: (a) TiO_2 1 min, TiO_2 5 min and TiO_2 10 min. (b) TiO_2 10 min/In_2O_3 5 s, TiO_2 10 min/In_2O_3 10 s, TiO_2 10 min/In_2O_3 20 s, TiO_2 10 min/In_2O_3 40 s, In_2O_3 10 s.

the highest amount of In_2O_3-sites exposed on the previously sputtered TiO_2 layers on the polyester.

The accelerated bacterial inactivation demonstrated for the TiO_2–In_2O_3 compared to the bare TiO_2 samples may be related to the favourable electrostatic attraction existing between the positive charged Ti and interacting with the *E. coli* negative surface at pH 7. The *E. coli* presents a negative charge between pH 3 and 9 due to the large amount of negative carboxylic groups compared to the positively charged functional groups: amide I and amide II on the bilayer cell membrane [6,14,17,19].

The TiO_2 bactericide inactivation mechanism has been already reported and widely discussed [14–19]. A mechanism for the TiO_2–In_2O_3 *E. coli* inactivation, involving interfacial transfer (IFCT) will be discussed in Section 3.6.

Fig. 3b reports the effect of the light intensity on the bacterial inactivation kinetics at 30 mW/cm^2 and 50 mW/cm^2. The results indicate the beneficial effect of an increase in the semiconductor charges interacting with the bacterial envelope, leading to a faster bacterial inactivation.

Fig. 3c shows repetition disinfecting performance by a TiO_2–In_2O_3 10 min–10 s sample up to the 5th cycle. The 8th cycle shows a loss of bacterial inactivation kinetics for applied doses of 30 mW/cm^2 and 50 mW/cm^2 due possibly to the leaching of the In and Ti-ions. This was confirmed by analysis performed by Inductively Coupled Plasma Mass Spectrometry ICP-MS on the sample TiO_2–In_2O_3 10 min–10 s at the end of recycling experiments (data not shown).

3.3. Diffuse reflectance spectroscopy (DRS) and visual appearance of the polyester coated samples

Fig. 4a shows the UV–vis reflectance spectra of TiO_2 sputtered for increasing times on polyester. The Kubelka–Munk (KM/S) relations convert reflectance measurements into absorption spectra units. K and S are the absorption and scattering coefficients respectively of TiO_2 in Fig. 4a. The KM/S values for the samples were found proportional to the TiO_2 sputtering time and finally related to the bacterial inactivation time reported in Fig. 2 for TiO_2 loaded samples. The faster bacterial inactivation induced by TiO_2–In_2O_3 in

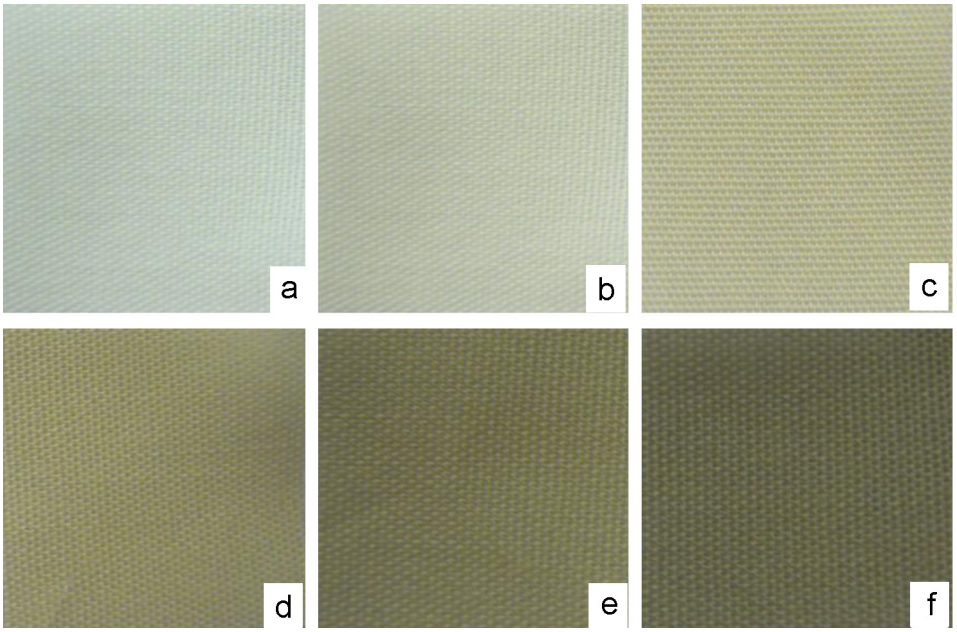

Fig. 5. Pictures of the magnetron sputtered polyester samples: (a) polyester alone, (b) TiO_2 10 min, (c) TiO_2 10 min–In_2O_3 5 s, (d) TiO_2 10 min/In_2O_3 10 s, (e) TiO_2 10 min–In_2O_3 20 s, (f) TiO_2 10 min–In_2O_3 40 s.

Fig. 3, suggests electronic transfer from In_2O_3 to TiO_2 intervening in bacterial inactivation.

Fig. 4b shows a progressive increase in optical absorption (KM/S spectra) in the region 350 nm. Samples sputtered with In_2O_3 for 5 to the 20 s sputtered show lower absorption intensities. But samples sputtered for 40 s, may lead to the formation of larger clusters of In_2O_3. Fig. 4b shows a weak absorption band from 400 to 500 nm, which can be attributed to the interfacial charge transfer (IFCT) from the TiO_2 to In_2O_3 layers. The weak absorption between 500 and 600 nm is due to the In_2O_3 inter-band indirect transitions at potential levels ≥2.09 eV [25]. These electronic transitions occur from the In_2O_3 valence band to two levels near the conduction band ≥2 eV [24]. The TiO_2–In_2O_3 transition seems to originate from the In_2O_3 (In5s5p orbital) to the conduction band of TiO_2 [24].

The visual appearance of TiO_2–In_2O_3 sputtered polyester surfaces is shown in Fig. 5. The light green colour is due to the In_2O_3 with a band gap of 2.5–2.8 eV (absorption edge of ~500–440 nm) becomes darker at longer sputtering times [25–28].

3.4. X-ray diffraction investigation of TiO_2 and TiO_2–In_2O_3 films

Fig. 6 shows the TiO_2 XRD pattern for bare TiO_2 and for In_2O_3/TiO_2 films, respectively. Fig. 6 presents the XRD diffractogram for the TiO_2 DC sputtered on polyester for 10 min. The intense anatase peak at 24.6° is due to the presence of anatase on the polyester. No specific signal due to In_2O_3 was detected in the XRD diffractogram, probably due to its very low loading (<0.2%). Only a slight decrease in intensity of the 24.6° (1 0 1) anatase peak was observed in the In_2O_3/TiO_2 sample. In addition no modification in the TiO_2 diffraction peaks due to In_2O_3 was detected, suggesting that no lattice doping takes place.

3.5. X-ray photoelectron spectroscopy (XPS) investigation

Fig. 7 shows the fitting of the Ti2p XPS envelopes for a TiO_2 10 min/In_2O_3 10 s sample at: (a) time zero and (b) after 300 min bacterial inactivation under an Osram Lumilux T8-L18W lamp. The Ti^{4+} doublet peak shift from 458.5 eV at time zero to 458.8 eV after the 300 min during bacterial inactivation suggests redox reactions

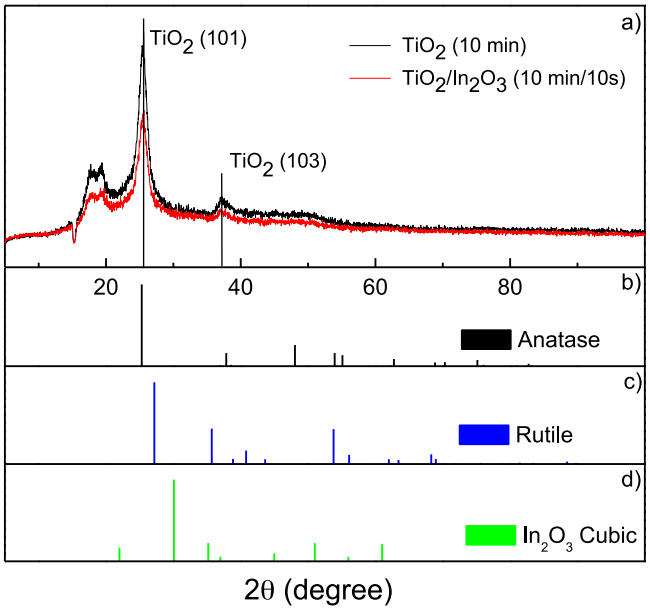

Fig. 6. XRD diffractograms of (1) TiO_2 10 min and (2) TiO_2 10 min/In_2O_3 10 s sputtered on polyester (a) diffraction patterns of anatase (b), rutile (c) and (d) cubic In_2O_3.

since the Ti^{4+} peak shift is ≥0.2 eV [30–32]. In Fig. 7a and b, a Ti^{3+} peaks shift is observed for the signal at zero and after 300 min from 457.8 eV to 458.9 eV. Samples of TiO_2–In_2O_3 show two peaks at 444 eV and 451 eV, respectively, assigned to $In3d_{5/2}$ and $In3d_{3/2}$ that also shifted during the bacterial inactivation by 0.3–0.4 eV (data not reported) [33–34].

3.6. Interfacial charge transfer mechanism (IFCT) in TiO_2–In_2O_3 composite films

Coupling TiO_2–In_2O_3 induced a significant increase in the photocatalytic activity compared to TiO_2 alone and In_2O_3. This significant increase is due to the positions of the conduction band (cb) and

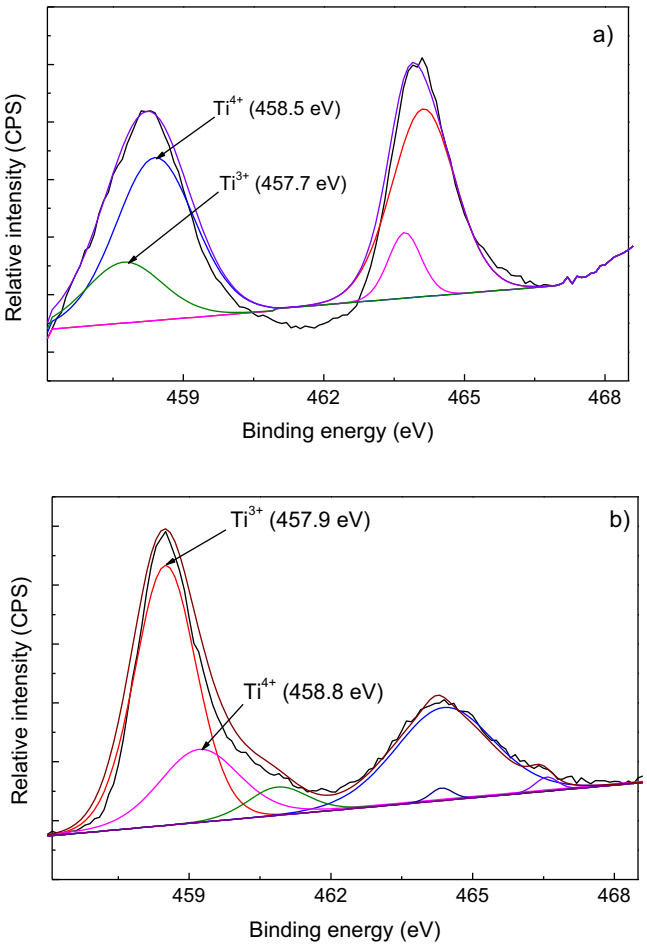

Fig. 7. Deconvolution of the Ti2p XPS envelope for a TiO_2 10 min/In_2O_3 10 s sample: (a) time zero and (b) after 300 min bacterial inactivation under Osram Lumilux T8-L18W lamp irradiation.

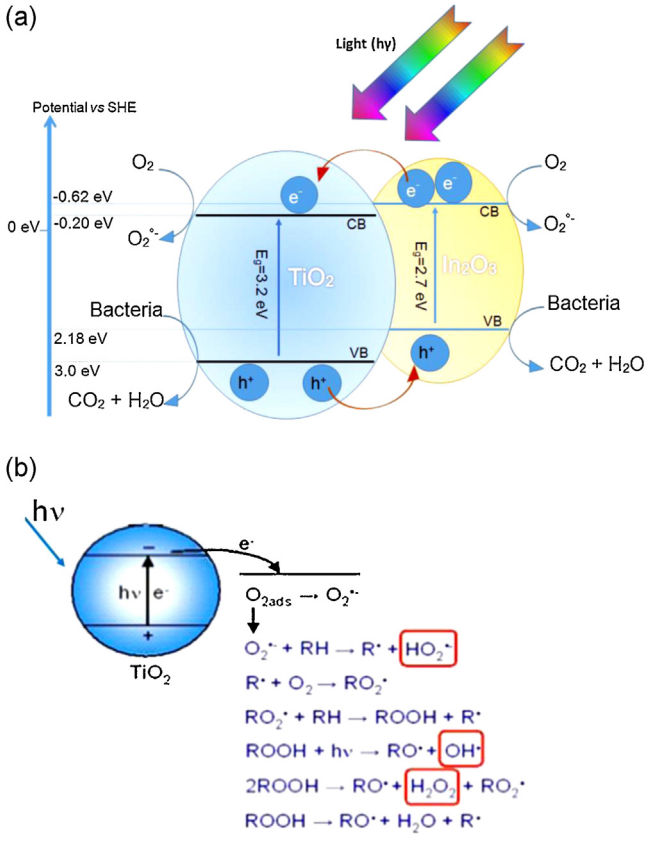

Fig. 8. (a) Scheme of the charge injection during the interfacial charge transfer (IFCT) between In_2O_3 and TiO_2 under simulated sunlight. (b) Radical(s) reaction generated from O_2 reduction on TiO_2 (R: bacteria degradation or species produced during the bacterial degradation).

valence band (vb) in In_2O_3 and TiO_2. The cb of In_2O_3 at −0.62 vs NHE [26–29] is able to transfer the cb electrons to TiO_2 (cb at 0.2 eV vs NHE for anatase). The UV component of sunlight can generate holes in TiO_2 at a level able to transfer the holes to In_2O_3 vb as suggested in Fig. 8a.

The subsequent spatial separation of photogenerated charge carries should limit the detrimental e^-/h^+ recombination events in TiO_2. The considerable difference in potentials between the two c, makes the In_2O_3 a good candidate for TiO_2 sensitization. The highly dispersed In_2O_3 on the TiO_2 layers, generating a Schottky barrier at the interface between TiO_2 and In_2O_3. This precludes in part the recombination of electrons and hole pairs. The scheme in Fig. 8a suggests the IFCT in the TiO_2–Tn_2O_3 assuming that the generated charges have a sufficient lifetime to diffuse to the surface inactivating bacteria. In this composite system TiO_2 is the main photocatalyst and the In_2O_3 acts as an additional visible light sensitizer.

Fig. 8b shows schematically the e^-_{cb} in the TiO_2 and In_2O_3 particles reacting with the adsorbed O_2 on the TiO_2 surface to yield $O_2^{-\bullet}$ radical anion and subsequently yielding other highly oxidative protonated radicals leading to bacterial inactivation.

4. Conclusions

TiO_2 and TiO_2–In_2O_3 layers were sputtered on polyester. Their bactericide kinetics was reported under actinic and solar simulated low intensity light. The addition of In_2O_3 on TiO_2 polyester shifts the optical absorption of TiO_2 into the visible region accelerating the bacterial inactivation kinetics compared to bare TiO_2. The In_2O_3 layer thickness and optical absorption was related to the bacterial inactivation kinetics. The photocatalytic surfaces were characterized by surface techniques as: XRF, DRS, XRD and XPS. The weak IFTC bands observed between 400 nm and 500 nm in TiO_2–In_2O_3 induced an increase in the quantum yield efficiency leading to a faster bacterial inactivation compared to bare TiO_2. TiO_2–In_2O_3 may be used in disinfecting textiles, taking into account that Ti and In are not toxic to human health, and readily available metals in nature.

Acknowledgments

We thank the financial support by the EPFL and the LIMPID FP7 Collaborative European Project Nanocomposite Materials for Photocatalytic Degradation of Pollutants NMP 2012.2.2.2-6 (n.310177). We also thank the COST actions MP 1101 and MP1106 for interactive discussions during the course of this study.

References

[1] Thüringer Surface and Biomaterials Kolloquium, 13–15 September 2011, Zeulenroda, Germany.
[2] K. Taylor, R. Roberts, J. Roberts, The Challenge of Hospital Acquired Infections (HAI), National Audit Office, 2002.
[3] R. Plowman, R. Graves, N. Griffin, L. Taylor, The rate and cost of hospital acquired infections, J. Hosp. Infect. 47 (2001) 198–204.
[4] S. Dancer, The role of the environmental cleaning in the control of hospital acquired infections, J. Hosp. Infect. 73 (2009) 378–386.
[5] A. Kramer, I. Schwebke, G. Kampf, How long do nosocomial pathogens persist in on inanimate surfaces? BMC Infect. Dis. 6 (2006) 137–146.

[6] A. Mills, C. Hill, P. Robertson, Overview of the current ISO tests for photocatalytic materials, J. Photochem. Photobiol. A 237 (2012) 7–23.
[7] K. Page, M. Wilson, P.I. Parkin, Antimicrobial surfaces and their potential in reducing the role of the inanimate environment in the incidence of hospital-acquired infections, J. Mater. Chem. 19 (2009) 3819–3831.
[8] S. Noimark, Ch. Dunnill, M. Wilson, P.I. Parkin, The role of surfaces in catheter-associated infections, Chem. Soc. Rev. 38 (2009) 3435–3448.
[9] C. Page, M. Wilson, N. Mordan, W. Chrzanowski, J. Knowles, P.I. Parkin, Study of the adhesion of *Staphylococcus aureus* to coated glass substrates, J. Mater. Sci. 46 (2011) 6355–6363.
[10] H.A. Foster, P. Sheel, W.D. Sheel, P. Evans, S. Varghese, N. Rutschke, M.H. Yates, Antimicrobial activity of titania/silver and titania/copper films prepared by CVD, J. Photochem. Photobiol. A. 216 (2010) 283–289.
[11] M.S.P. Dunlop, P.C. Sheeran, A.J.M. Byrne, S.A. McMahon, M.A. Boyle, G.K. McGuigan, Inactivation of clinically relevant pathogens by photocatalytic coatings, J. Photochem. Photobiol. A. 216 (2010) 303–3010.
[12] M.H. Yates, A.L. Brook, B.I. Ditta, P. Evans, H.A. Foster, D.W. Sheel, A. Steele, Photo-induced self-cleaning and biocidal behaviour of titania and copper oxide multilayers, J. Photochem. Photobiol. A. 197 (2008) 197–2008.
[13] I.M. Mejia, M. Marín, R. Sanjines, C. Pulgarín, E. Mielczarski, J. Mielczarski, J. Kiwi, Magnetron-sputtered Ag-modified cotton textiles active in the inactivation of airborne bacteria, ACS Appl. Mater. Interfaces 2 (2010) 230–235.
[14] W. Tung, W. Daoud, Self-cleaning fibers via nanotechnology: a virtual reality, J. Mater. Chem. 21 (2011) 7858–7870.
[15] L. Zhang, R. Dillert, D. Bahnemann, M. Vormoor, Photoinduced hydrophilicity and self-cleaning: models and reality, Energy Environ. Sci. 5 (2012) 7491–7507.
[16] O. Dalrympe, E. Stefanakos, M. Trotz, Y. Goswamy, A review of the mechanisms and modelling of photocatalytic disinfection, Appl. Catal. B. 98 (2010) 27–38.
[17] H. Foster, I. Ditta, S. Varghese, A. Sreele, Photocatalytic disinfection using titanium: spectra and mechanism of antimicrobial activity, Appl. Microb. Biotechnol. 90 (2011) 184–186.
[18] A. Fujishima, T. Rao, D. Trick, Titanium dioxide photocatalysis, J. Photochem. Photobiol. C: Rev. 1 (2000) 1–21.
[19] A. Fujishima, K. Hashimoto, T. Watanabe, TiO_2 Photocatalysis Fundamentals and Applications, Bkc Inc., Tokyo, 2000.
[20] S. Rtimi, O. Baghriche, R. Sanjines, C. Pulgarin, M. Bensimon, J. Kiwi, TiON and TiON-Ag sputtered surfaces leading to bacterial inactivation under indoor actinic light, J. Photochem. Photobiol. A: Chem. 256 (2013) 52–63.
[21] X. Qiu, M. Miyaguchi, K. Sunada, M. Minoshima, M. Liu, Y. Lu, D. Li, Y. Shimodaira, Y. Hosogi, K. Ykuroda, 1. Hashimoto, Hybrid Cu_x/TiO_2 nanocomposites as risk-reduction materials in indoor environments, ACS Nano 6 (2012) 1609–1618.
[22] O. Baghriche, S. Rtimi, R. Sanjines, C. Pulgarin, J. Kiwi, Effect of the spectral properties of TiO_2, Cu, TiO_2/Cu sputtered films on the bacterial inactivation under low intensity actinic light, J. Photochem. Photobiol. A 251 (2013) 50–56.
[23] S. Rtimi, O. Baghriche, C. Pulgarin, R. Sanjines, J. Kiwi, Innovative TiO_2/Cu surfaces inactivating bacteria <5 min under low intensity visible/actinic light TiO_2/Cu surfaces, ACS Appl. Mater. Interfaces 4 (2012) 5234–5240.
[24] N. Novkovski, A. Tanusevski, Origin of the optical absorption of In_2O_3 thin films in the visible range, Semicond. Sci. Technol. 23 (2008) 095012.
[25] J.B. Mathews, Epitaxial Growth Part B, IBM Thomas Watson Research Center, Academic Press, New York, 1975, pp. 382–436.
[26] A. Chakraborty, M. Kebede, Efficient decomposition of organic pollutant over In_2O_3/TiO_2 nanocomposite photocatalyst under visible light irradiation, J. Cluster Sci. 23 (2012) 247–257.
[27] F. Ma, S. Zhang, X. Yang, W. Guo, M. Huo, Fabrication of metallic platinum and indium oxide codoped titania nanotubes for the simulated sunlight photocatalytic degradation of diethyl phthalate, Catal. Commun. 24 (2012) 75–79.
[28] J.F. McCann, J. O'M Bockris, Determination of electrochemical parameters of semiconductor materials, J. Electrochem. Soc. 128 (1981) 1719–1724.
[29] W. Erbs, J. Kiwi, M. Gratzel, Light induced oxygen generation in aqueous dispersions of In_2O_3 particles and determination of their conduction band position, Chem. Phys. Lett. 110 (1984) 648–650.
[30] C.D. Wagner, E.L. Davis, G.E. Müllenberg (Eds.), Handbook of X-Ray Photoelectron Spectroscopy, Perkin-Elmer, Minnesota, 1979.
[31] D.A. Shirley, corrections of electrostatic species in SP-spectroscopy, Phys. Rev. B 5 (1972) 4709–4714.
[32] J. Nogier, M. Delamar, M. Grätzel, K. Thampi, J. Kiwi, X-ray photoelectron spectroscopy of V_2O_5/TiO_2 catalysts, Catal. Today 20 (1994) 109–124.
[33] C. Donley, D. Dunphy, D. Paine, C. Carter, K. Nebesny, P. Lee, D. Alloway, N.R. Armstrong, Characterization of indium–tin oxide interfaces using X-ray photoelectron spectroscopy and redox processes of a chemisorbed probe molecule: effect of surface pretreatment conditions, Langmuir 18 (2001) 450–457.
[34] W.J. Tseng, T.T. Tseng, H.M. Wu, Y.C. Her, T.J. Yang, Facile synthesis of monodispersed In_2O_3 hollow spheres and applications in photocatalysis and gas sensing, J. Am. Ceram. Soc. 96 (2013) 719–772.